Journal of Heat and Mass Transfer Research

Journal homepage: http://jhmtr.semnan.ac.ir

Semnan University

Transient Simulation and Life Cycle Cost Analysis of a Solar Polygeneration System Using Photovoltaic-Thermal Collectors and Hybrid Desalination Unit

Maryam Karami [*,a], Seyedeh Somayeh Nasiri Gahraz[a]

[a]*Department of Mechanical Engineering, Faculty of Engineering, Kharazmi University, Tehran, Iran.*

PAPER INFO

Paper history:
Received: 2021-05-15
Revised: 2021-09-24
Accepted: 2021-10-10

Keywords:
Solar polygeneration system;
Photovoltaic-thermal solar collectors;
Humidification-Dehumidification (HDH);
Reverse Osmosis;
Hot-Dry climate;
Economic analysis.

ABSTRACT

Recently, water scarcity has been intensified in arid areas because of depletion of freshwater resources, reduction of rainfall, population, and urbanization growth. Therefore, the need to use desalination systems has increased in these areas. On the other hand, the increase of building energy consumption for achieving enhanced thermal comfort has become a global crisis due to the depletion of fossil fuel resources and related environmental problems. In this study, a small-scale solar polygeneration system using photovoltaic-thermal solar collectors and hybrid humidification-dehumidification and reverse osmosis desalination units is proposed to supply the electricity, domestic hot water, space heating, and freshwater demands of a one-story house. The dynamic simulation of the system performance in the Hot-Dry climate zone is done using the TRNSYS-MATLAB co-simulator. The results indicate that using the thermal and electrical energy generated by the proposed system, the building annual energy consumption for providing domestic hot water, and space heating demands reduce 100% and 27.2%. The increase of the annual solar fraction of domestic hot water and space heating, because of using the electrical energy generated by the system, is 11.3% and 15.6%, respectively. The electricity and freshwater demand of the building is completely supplied by the proposed system and the excess electricity is sold to the grid. Economic analysis indicated that fuel saving cost of 29479 $ and water saving cost of 23779 $ are obtained during the life cycle of the system and the payback period is 3.75 years. The results show that the considerable energy savings are achieved using the proposed solar polygeneration system for providing the required electricity, heating, and fresh water demands of the residential buildings.

DOI: 10.22075/JHMTR.2021.23429.1343

1. Introduction

The use of renewable energy as an alternative to fossil fuels has been one of the challenges of energy policymakers in the present century. Besides the environmental and economic benefits of renewable energy, the energy consumption growth and excessive use of fossil fuels cause that the attention to renewable energy has increased in different countries. Among various forms of renewable energy, solar energy, which is harvested through solar photovoltaic (PV) panels [1] and solar collectors [2], presents a great prospect and opportunity for reducing the amount of energy consumption and also, the environmental pollution arising from the use of fossil fuels [3].

One of the major problems of PV panels is the high temperature of the absorber plate, which leads to reduce the efficiency of PV panels [4]. Nowadays the combination of photovoltaic and thermal (PVT) solar collectors, as one of the most common methods for cooling PV panels, which generate the electrical and thermal energy simultaneously, are a promising technology for cost-effective collecting the solar energy [5, 6]. The heat from the PV panels is transferred to the working fluid and is used in low temperature applications such as solar combisystems (SCS) to supply domestic hot water (DHW)

[*]*Corresponding Author: Maryam Karami, Department of Mechanical Engineering, Faculty of Engineering, Kharazmi University, Tehran, Iran.*
Email: karami@khu.ac.ir

and space heating (SH) demands or thermal desalination systems to produce distilled water (DW).

There are numerous studies about the thermal performance of PVT-based SCS. The study on DHW and electricity production by PVT collectors, done by Dupeyrat et al. [7], showed that the thermal energy savings of 55% require a water-cooled PVT area of 6.2 m^2 for the climatic conditions of Paris. Liang et al. [8] studied supplying the SH demand by an SCS based on PVT collectors and floor heating system using TRNSYS. They found that by using a PVT collector area of 32 m^2, the proposed system can achieve an annual power output of 131 kWh and the variation of indoor temperature ranges from 16.3℃ to 19.5℃ on a typical day. Hazami et al. [9] performed an energy and exergy analysis of a PVT-based SCS to produce DHW and electrical demands for a building in Tunisia. The experimental results indicated that the maximum instantaneous thermal and electrical energy efficiency were about 50% and 15%, respectively. It was also found that the maximum thermal and electrical exergy efficiencies were about 50% and 14.8%, respectively. Based on the simulation results, about 14.6% and 5.33% of the DHW and electrical demands of the building are obtained using the proposed system. In the next study, Hazami et al. [10] investigated the thermal performance of a PVT-based SCS, which provides the DHW, SH and electrical demands of a typical Tunisian building with an area of 120 m^2. They reported that the system provided between 20% and 45% of the SH demand and between 40% and 70% of the DHW demand. Economic analysis of the system indicated that the annual energy saving and the payback period were 7618.3 kW h/year and 10.2 years, respectively. Herrando et al. [11] optimized the PVT-based SCS for the simultaneous production of DHW, SH, and electricity for a single-family home at three locations including Athens (Greece), London (UK), and Zaragoza (Spain). They pointed out that the optimized system provides 65% of the annual electricity demands in Athens, London, and Zaragoza using the collector areas of 14.0 m^2, 17.0 m^2, and 12.4 m^2, respectively. The total DHW and SH demands of 60%, 45%, and 30% are provided by the system in Athens, Zaragoza, and London, respectively. Using Polysun software simulation, Elmnifi et al. [12] reported that the annual savings of 1895 dollars and the reduction of carbon dioxide emissions of 15447 kg are obtained PVT-based SCS by using in Northeastern Libya.

Solar energy is also a relatively simple solution to the water crisis so that has the maximum share of 51% of worldwide renewable desalination capacity [13]. Solar desalination systems are widely used in areas with higher solar irradiance, where more water scarcity is expected [14]. In recent years, PVT collectors have been extensively used to produce DW by desalination of saline water. The desalination process is the process of purifying saline water for drinking purposes. A desalination system generally divides saline water into two streams: a pure stream with a very small percentage of salts, or a DW stream and a stream containing residual salts. Separating salt from saline water is a thermodynamic process that requires energy. Solar desalination systems use both direct and indirect solar energy to produce freshwater [15, 16]. In a direct type of solar desalination unit, which is called solar still, the heat of the Sun is used to drive evaporation from humid soil, and ambient air to cool a condenser film [17]. The indirect solar desalination systems use either electricity generated by photovoltaic cells such as reverse osmosis (RO), electrodialysis, membrane distillation, or thermal energy generated by solar collectors such as multi-stage flash (MFS), multi-effect distillation (MED), vapor compression (VC) and humidification-dehumidification (HDH).

In recent years, researchers have shown great attention to indirect solar desalination systems using PVT collectors. By the exergeoeconomic analysis of a solar thermal/desalination combisystem, Calise et al. [18] showed that the exergy efficiency of all major components except the concentrating photovoltaic/thermal (PVT) collector is slightly reduced during the central hours. They also found that the distilled water (DW) production increases using the multiple distillation method and the system cost reduces by 1.6%. Monjezi et al. [19] studied the performance of an off-grid combined PVT-RO desalination system, in which seawater is used as the cooling medium of PV panels to increase the thermal efficiency of PV panels and thus, DW production rate. The reduction of the electricity consumption rate of RO desalination and required PV panel surface area are the results of the combined system. Alqaed et al. [20] used PVT collectors for generating the required electricity of the pumps and thermal energy to preheat the feedwater of RO, which results in the reduction of pumping power because of the viscosity decrease of feedwater. The results show that the annual cost of the plant using the PVT-RO system is 18% lower than that using conventional electricity.

There are also some studies on the thermal performance of combined PVT-HDH systems. The HDH is based on the fact that air has capable of carrying a significant amount of water vapor. When air comes into contact with saline water, some water is vaporized and absorbed by the air. This steam can be distilled and recycled by passing from cold surfaces to produce distilled water [21]. Giwa et al. [22] investigated the integrated air-cooled PVT system with ambient seawater inflow into an HDH desalination system. Their results indicated that a daily average of 2.28 L of freshwater produces per m^2 of PVT collectors. Compared to the PV-RO system, the PVT-HDH system resulted in an 83.6% decrease in environmental impacts. By the numerical simulation of the PVT-HDH system, Hosseini and Sarhaddi [23] reported that the increase of the number of PVT panels increases the produced DW and electricity, but thermal efficiency decreases because of the pumping power increase. The increase of saline water temperature has a negative effect on the electrical and thermal efficiency and also, reduces the produced DW. In

a similar study, Anand and Srinivas [24] investigated the effect of mass flow rate on the performance of the PVT-HDH desalination system using a mathematical model in MATLAB. They found that by increasing the mass flow rate, the electrical efficiency increases, whereas the total efficiency decreases. The highest electrical and total efficiency of 16.6% and 43.2% are obtained at a mass flow rate of 110 kg/h and 30 kg/h, respectively. The highest DW production rate (0.82 L/h) was also achieved at a mass flow rate of 30 kg/h. Mostafavi et al. [25] studied the thermal performance of a PVT-HDH in various air velocities (1, 1.5, and 2 m/s) and brackish water rates (94, 189, and 283 kg/h) using an experimental setup. The results show that the maximum DW produced is about 4.2 kg/day at a brackish water rate of 189 kg/h and an air velocity of 1 m/s. Elsaf [26] integrated an HDH desalination system with concentrated PVT collectors (CPVT) for simultaneous DW and electricity production. The results show that the system would be able to produce 12 m^3 DW and 960 kWh of electricity per year for a site with a solar irradiance of 1.88 MWh/yr. Gabrielli et al. [27] optimized the performance of HDH-PVT collators and found that the DW production is maximized at the highest possible saline water flow rate depending on the PVT configuration and the ambient conditions. In an interesting work, Otanicar and Weilin [28] investigated thermodynamic analysis of hybrid HDH/RO desalination systems powered by CPVT collectors. The results show that a hybrid HDH/RO system utilizing both thermal and electrical energy can produce 38% more DW at steady state conditions than by utilizing the entire solar collector output as electrical energy for powering a stand-alone RO system.

The literature review reveals that the small-scale solar polygeneration system based on flat-plate PVT and hybrid HDH/RO units has not been yet investigated. Therefore, in this paper, for the first time, the thermal performance of a solar polygeneration system is investigated to simultaneously generate the electricity, DHW, SH, and freshwater demands of a one-story house. To produce the DW, both solar thermal and electrical energy generation by PVT collectors are used by the hybrid HDH/RO units. The system simulation is done for the climatic conditions of Isfahan, which is located in the Hot-Dry climate zone of Iran. In some cities of this province, due to excessive use of groundwater, people have reached salty water and the nitrate is entered into the water. Therefore, using water desalination systems has become inevitable. Finally, the economic analysis of the proposed system is also performed using the life cycle analysis method.

2. System description and modeling

2.1. Solar polygeneration system

The schematic of the proposed solar polygeneration system is indicated in Figure 1. An array of PVT solar collectors is used to supply the required thermal energy which is divided between the DHW, SH, and DW storage tanks using a flow diverter (FD1). The electrical energy generated by the PVT collector is used to supply the electrical demand and to produce DW by RO unit. The DW production scenario is that if the DW produced by the HDH unit is not enough, the electricity produced by the system is used to produce the rest of the freshwater demand using RO units. Finally, the excess electricity is used to meet the electrical demand. Three storage tanks, one for DHW, one for SH, and another for DW are used in the system. If needed, the auxiliary electrical heaters, embedded in the DHW and SH tanks, are used to supply the demands. In this study, the electricity required by the electrical auxiliary heaters is first supplied by the excess electricity generated by the system. The rest of the electricity needed by the DHW auxiliary heater is supplied by the grid, while a gas-fired boiler is used as an auxiliary heater for supplying the rest of SH demand, which only turns on during the cold months. If there is no SH demand, the thermal energy produced by PVT collectors is directed to the DW tank using a flow diverter (FD2). In this system, an HDH system including a humidifier (HUM) and a dehumidifier (DHUM) is used for water desalination. Two mixing valves (MV1 and MV2) are used to mix the return flows from the tanks before entering the solar collectors.

2.2. TRNSYS simulation model

Figure 2 indicates the TRNSYS model of the proposed solar polygeneration system. The features and TRNSYS types of the components used to simulate the system are listed in Table 1. As mentioned, in the case of generated thermal energy, the control strategy is set up to supply the DHW demand and then, the excess thermal energy is used to provide the SH demand and if there is no SH demand, it is used to produce the DW. In other words, all the thermal energy absorbed by the solar collectors is allocated to the DHW storage tank and DW storage tank in the warm months. In the case of generated electrical energy, the priority is supplying the DW demand and then, supplying the electrical demand. The excess electrical energy is used to provide the need for DHW and SH auxiliary heaters.

Using the results of the simulation, the performance indicators of the proposed system can be determined. The DHW solar fraction (DHWSF) and SH solar fraction (SHSF) is defined as the ratio of energy supplied by solar energy to the required energy, given by the following relations:

$$DHWSF = 1 - \frac{Q_{aux.DHW}}{Q_{DHW\ demand}} \quad (1)$$

$$SHSF = 1 - \frac{\mathrm{Q_{aux.SH}}}{\mathrm{Q}_{SH\ demand}} \quad (2)$$

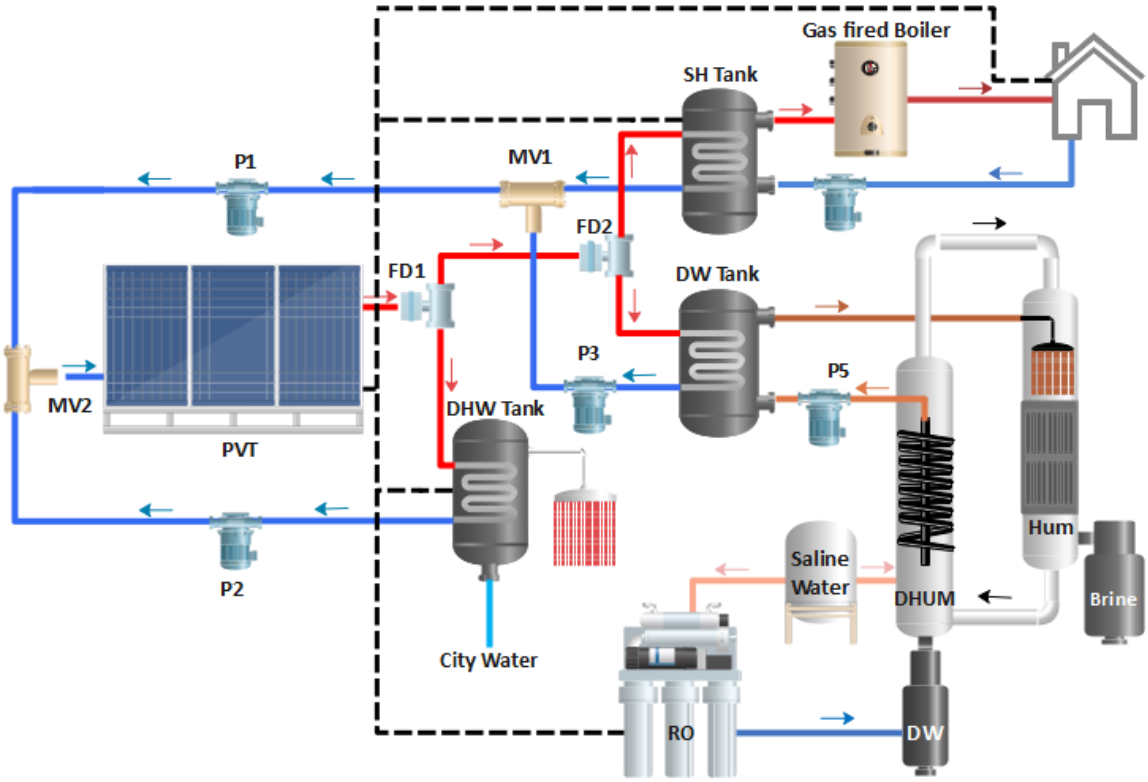

Figure 1. Schematic of the proposed solar polygeneration system

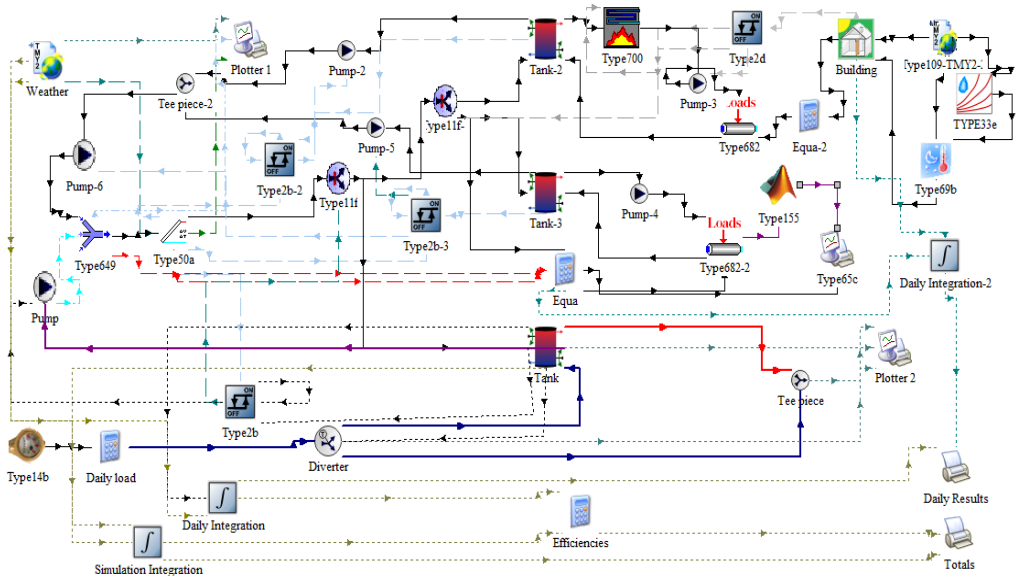

Figure 2. Descriptive diagram of TRNSYS model of the proposed solar polygeneration system

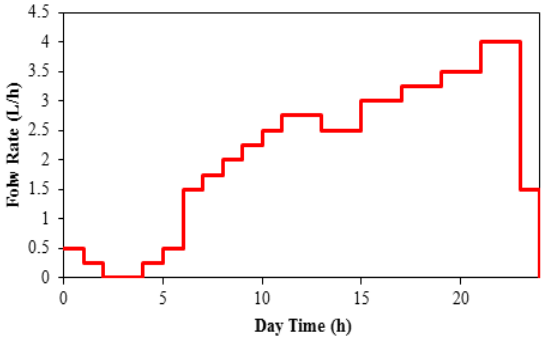

Figure 3. Daily DHW consumption profile [29]

Table 1. Features and TRNSYS types of the main components used in the simulation

Model	Features
Building	Type 56 Floor area: 100 m^2 Height: 2.8 m Overall heat transfer coefficient of external walls: 0.27 W/m2K Overall heat transfer coefficient of roof: 0.27 W/m2K Overall heat transfer coefficient of windows: 1.27 W/m2K Inside set point temperature: 26℃ Occupants: 4 persons, seated, light work Natural ventilation: 1 AC/h Infiltration: 0.16 AC/h Artificial lighting: 5 W/m2 Window-to-Wall Ratio (WWR): 30% DHW demand: 50 lit/person.day
Weather information	Type 109 Weather information is obtained from METEONORM software. The effective sky temperature is calculated by Type 69. Psychometric properties such as dew point temperature, relative humidity, etc. are calculated by Type 33.
PVT collectors	Type 50a Collector area: 18 $\mathbf{m^2}$ Collector flowrate: 40 $kg/h.m^2$ Collector fin efficiency factor: 0.96 Collector loss coefficient: 16 $kJ/hr.m^2.K$ Temperature coefficient of solar cell efficiency: 0.0032 Packing Factor: 0.8
Storage tank	Type 4c Storage tank volume: 300 l (DHW), 800 l (SH), and 200 l (DW) Heat transfer coefficient of tank: 0.7 W/$\mathbf{m^2}$K Maximum power of internal electrical heater for DHW tank: 3.33 kW
Circulation pump	Type 3b Power coefficient: 0.5 Maximum power: 1 kW
Controller	Type 2b Controller type: Feedback controller
Flow diverter	Type 11f
DHW	Type 14b Operating temperature: 60℃ Figure 3 shows the DHW consumption profile.
Boiler	Type 700 Rated capacity: 15 kW Set point temperature: 80℃ Boiler efficiency: 0.78
Loads	Type 682

2.2.1 HDH modeling

In this paper, the HDH desalination system is used for producing DW. Figure 4 shows the components of a closed air open water (CAOW) HDH desalination system. Since the TRNSYS software is not able to simulate desalination, the governing equations on the performance of the HDH desalination system are coded in MATLAB and then, are coupled with the TRNSYS model using Type 155 to determine the produced DW by the STDSC. The assumptions of the HDH modeling are as follows:

- Steady state conditions.

- Potential and kinetic energy changes are negligible.
- No heat loss from humidifier and dehumidifier.
- The outlet water temperature from the condenser is assumed to be the average of inlet and outlet air temperatures.
- The air at the outlet of the humidifier and dehumidifier is saturated.

Considering the dehumidifier as a control volume, the mass, and energy conservation equations are written as follows [30]:

$$\dot{m}_{pw} = \dot{m}_a(\omega_{a.2} - \omega_{a.1}) \tag{3}$$

$$\dot{m}_w(h_{w,1} - h_{w,0}) + \dot{m}_{pw}h_{pw} = \dot{m}_a(h_{a,2} - h_{a,1}) \tag{4}$$

The mass and energy conservation equations for the humidifier are written as follows [30]:

$$\dot{m}_w - \dot{m}_a(\omega_{a.2} - \omega_{1.a}) = \dot{m}_b \tag{5}$$

$$\dot{m}_a(h_{a.1} - h_{a.2}) = \dot{m}_b h_{w.3} - \dot{m}_w h_{w.2} \tag{6}$$

The heat transfer from the collector to the fluid is obtained by using the following equation:

$$\dot{Q}_{heater} = \dot{m}_w c_{p.w}(T_{w.2} - T_{w.1}) \tag{7}$$

The enthalpy and relative humidity of the air are calculated as a function of the air flow temperature using the following relations [31]:

$$h = 0.005853T^3 - 0.497T^2 + 19.87T - 207.61 \tag{8}$$

$$\omega = 2.19 * 10^{-6}T^3 - 1.85 * 10^{-4}T^2 + 7.06 * 10^{-3}T - 0.077 \tag{9}$$

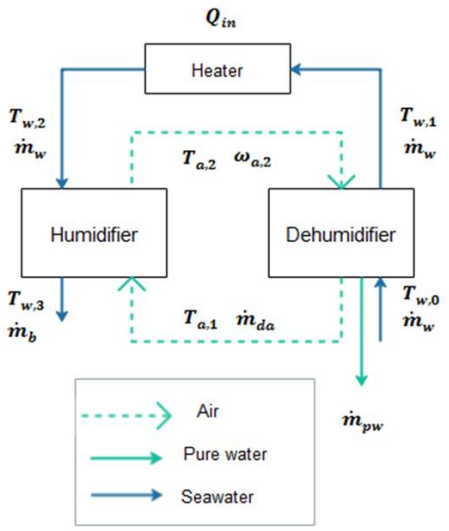

Figure 4. Schematic of a CAOW-HDH desalination system

The effectiveness of the heat exchanger can be defined as [26]:

$$\varepsilon = \frac{\Delta\dot{H}}{\Delta\dot{H}_{max}} \tag{10}$$

where $\Delta\dot{H}$ is the enthalpy changes of cold or hot fluid and $\Delta\dot{H}_{max}$ indicates the maximum enthalpy change that the fluid can achieve it.

Since the humidifier and the dehumidifier act as a heat exchanger, the following relations can be used for calculating the effectiveness the humidifier and the dehumidifier, respectively.

$$\varepsilon_H = \max\left(\frac{h_{a.out} - h_{a.in}}{h_{a.out.ideal} - h_{a.in}}, \frac{h_{w.in} - h_{w.out}}{h_{w.in} - h_{w.out.ideal}}\right) \tag{11}$$

$$\varepsilon_D = \max\left(\frac{h_{a.in} - h_{a.out}}{h_{a.in} - h_{a.out.ideal}}, \frac{h_{w.in} - h_{w.out}}{h_{w.in} - h_{w.out.ideal}}\right) \tag{12}$$

There are five unknowns ($T_{a.1}.T_{a.2}.T_{w.1}.T_{w.2}.T_{w.3}$), which can be calculated by solving Eqs. (3), (5), (6), (9), and (10) using the iterative solution method. The inputs are the inlet water temperature, the air temperature, the water flowrate, the air flowrate, the inlet heat rate. It is assumed that there is no temperature difference between inlet and outlet flows of the chamber for calculating ideal enthalpy difference. In other words, $T_{in.w} = T_{a.out.ideal}$ and $T_{in.a} = T_{w.out.ideal}$. Figure 5 shows the flowchart of the HDH modeling process.

The results of the HDH model are compared with the results of the experimental study [30]. The features of the experimental study [30] are entered to the developed model for considering the model validation. Table 2 indicates the measured and calculated gained output ratio (GOR) of the HDH in different saline water inlet temperature. The GOR is defined as:

$$GOR = \frac{\dot{m}_{fw}.h_{fg}}{Q_{in}} \tag{13}$$

where $\dot{m}_{fw}$, h_{fg} and Q_{in} are fresh water mass flow rate, evaporation enthalpy and inlet thermal energy to the HDH. As can be seen in Table 2, the experimental and numerical results were in good agreement by the maximum error of 7%.

2.2.2 Reverse osmosis

RO process is a form of pressurized filtration in which the filter is a semi-permeable membrane that allows water, but not salt, to pass through. RO unit sizes vary from a very small unit with a capacity of 0.1 m^3/day to a 395,000 m^3/day plant. The average reported energy consumption ranges from 3.7 to 8 kWh/m^3 [32]. In this study, the following relation is taken into account for calculating the distilled water by the RO unit:

$$\dot{m}_{DW.RO} = \frac{Electrical\ power\ (kWh)}{5} \tag{14}$$

Table 2. Comparison of the experimental and numerical results

Saline water inlet temperature (℃)		**60**	**70**	**80**	**90**
GOR	Present study	1.68	1.29	1.1	0.99
	Narayan et al. [30]	1.81	1.40	1.17	1.03

The efficiency of the RO unit is considered 50%.

3. Results and discussion

Figure 6 shows the monthly average solar irradiation and ambient temperature in Isfahan. The maximum and minimum ambient temperatures are 29.5℃ and 2.9℃ in July and January, respectively; while, the maximum and minimum solar irradiation are 459.2 W/m^2 and 782.6 W/m^2 in February and October, respectively.

The hourly variations of PV cell temperature, electrical and thermal efficiency are shown in Figure 7. It can be seen that the electrical efficiency decreases from 11.3% at 9:00 am to 9.95% at 13:30, then increases to 11% at 16:00. This is because the PV cell temperature increases from 38.7ºC at 9 am to 63ºC at 13:30, and then decreases to 42.8ºC at 16:00. As the temperature of the cell increases, the electrical efficiency decreases to its minimum value at the maximum cell temperature between 12:30 and 13:30. Looking at Figure 7, it is found that the thermal efficiency decreases from 56% at 9:00 am to 52.8% at 13:30, then increases to 59.2% at 16:00. The maximum and minimum total PVT efficiencies are 62.8% at 13:30 pm and 70.3% at 16:00.

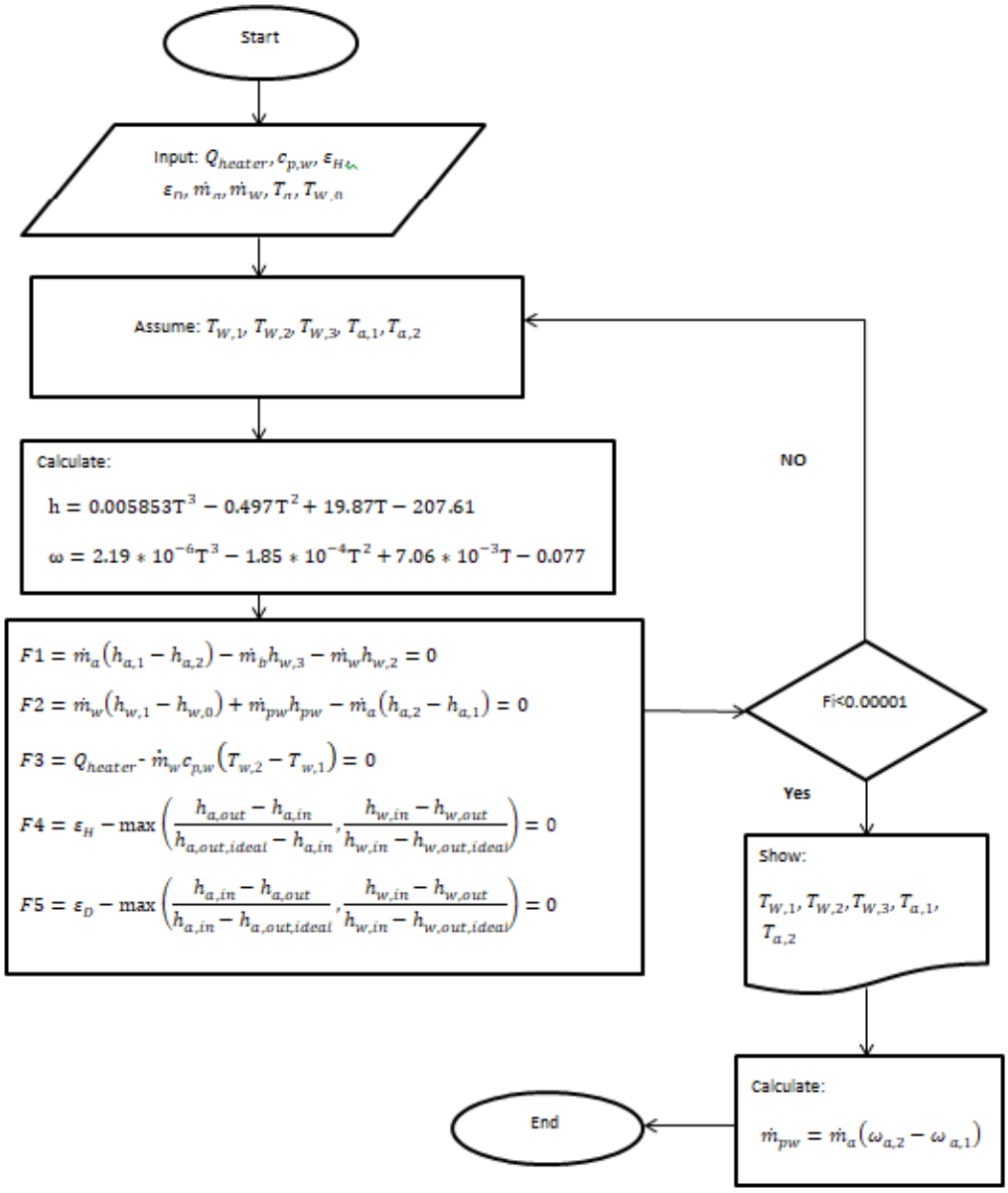

Figure 5. Flowchart of the HDH modeling process

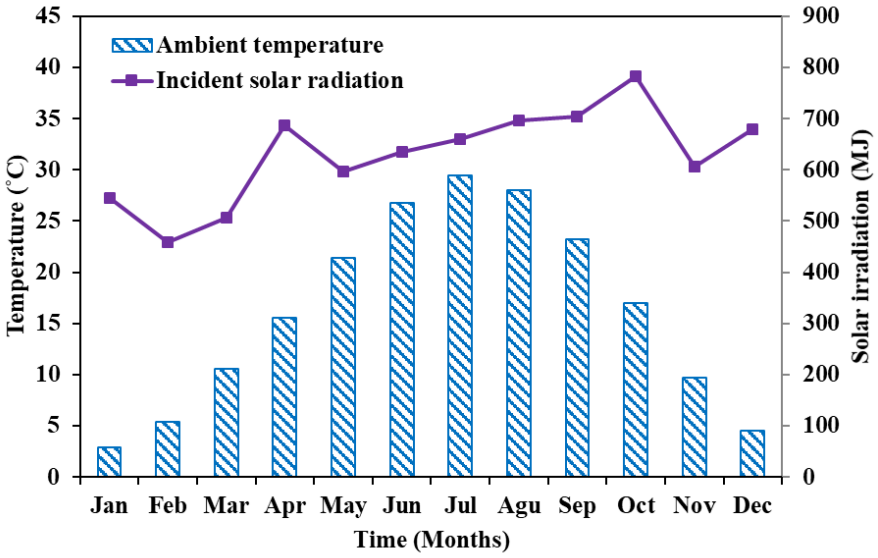

Figure 6. Monthly variations of ambient temperature and solar radiation

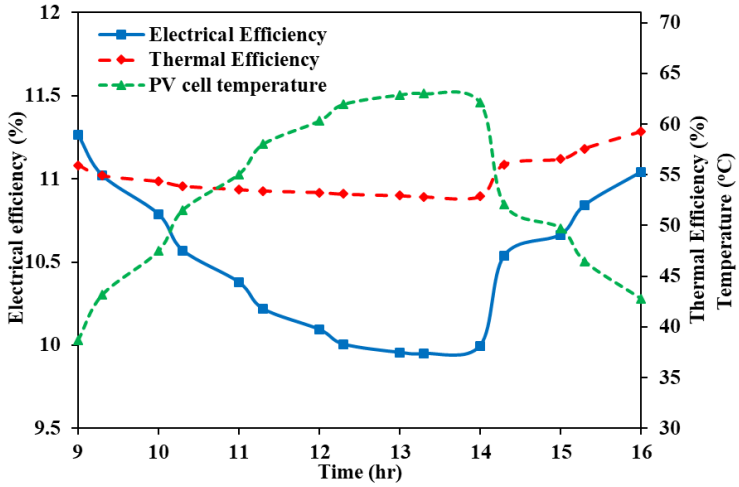

Figure 7. Hourly variations of electrical and thermal efficiency and PV cell temperature

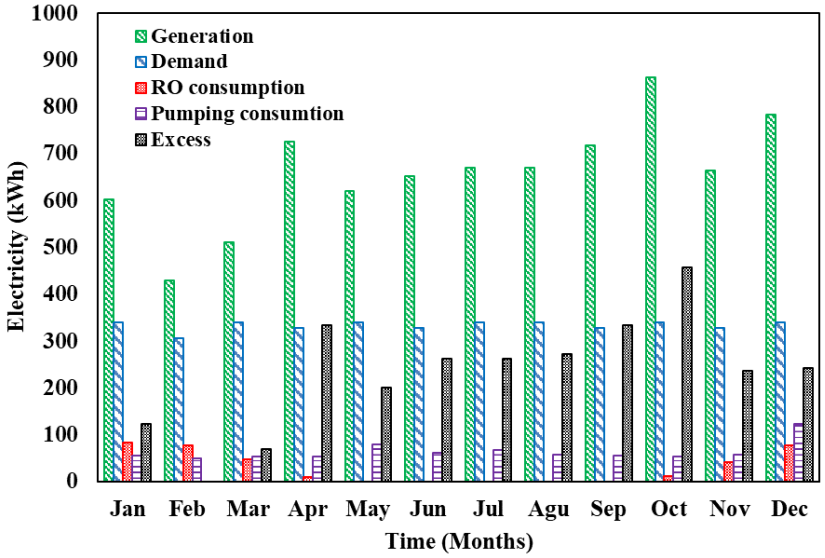

Figure 8. Monthly variations of the electricity generation and demand

In Figure 8, the monthly electricity demand of the house and generation by PVT collectors are plotted. As observed, the generated electricity is higher in the warm months, which have higher solar irradiation. The maximum and minimum electricity generation occur in October and February, which are 863 kWh and 428.7 kWh, respectively. It is found that in all months, the electricity generation can provide the electricity demand of the house and the excess electricity can be sold. The highest and lowest excess electricity is obtained in February (28.4%) and in October (60.6%), respectively. In February, the electricity consumed to produce DW by RO is maximum and about 18% of the system electricity generation, whereas in April, this value is minimum and about 1.3%. The maximum and minimum pumping electricity consumption is 80.15 kWh in April and 48.85 kWh in February. In October, when there is the maximum electricity generation and the RO electricity consumption is low, the maximum excess electricity of 443 kWh is obtained.

The monthly variation of the DHW demand and supply, and also, DHWSF is plotted in Figure 9. As observed, the DHW supply by the thermal solar energy is larger than the DHW demand in some months; however, there is a need to the DHW supply by the electrical energy. It is interesting to note that the auxiliary energy is still required in all months, even in which the supplied energy by solar radiation is higher than the required energy. For example, the auxiliary energy of about 4.84 MJ/m^2, which is supplied by the electrical energy generated by the system, is required for DHW supplying in March, while the DHW supply by thermal energy is higher than the DHW required energy in the same month. This is because of the temperature decrease of the storage tank when there is no solar radiation at night or cloudy weather. The maximum DHW supply by electrical energy, which shows the value of the required auxiliary energy, is occurred in January, which is 13.85 MJ/m^2. As observed, by using both thermal and electrical energy generated by the system, the DHWSF is 100% in all months.

The monthly variation of the DHW demand and supply, and also, DHWSF is plotted in Figure 9. As observed, the DHW supply by the thermal solar energy is larger than the DHW demand in some months; however, there is a need to the DHW supply by the electrical energy. It is interesting to note that the auxiliary energy is still required in all months, even in which the supplied energy by solar radiation is higher than the required energy. For example, the auxiliary energy of about 4.84 MJ/m^2, which is supplied by the electrical energy generated by the system, is required for DHW supplying in March, while the DHW supply by thermal energy is higher than the DHW required energy in the same month. This is because of the temperature decrease of the storage tank when there is no solar radiation at night or cloudy weather. The maximum DHW supply by electrical energy, which shows the value of the required auxiliary energy, is occurred in January, which is 13.85 MJ/m^2. As observed, by using both thermal and electrical energy generated by the system, the DHWSF is 100% in all months.

In Figure 10, the system performance is evaluated in terms of SHSF, the SH demand, supply, and auxiliary energy. The results show that the SH demand varies from 56.2 MJ/m^2 in November to 214.8 MJ/m^2 in January. As can be seen, the SHSH is obtained between %11-%100 in cold months; therefore, the most fraction of the SH demand should be provided by the auxiliary heater in these months. As can be seen in Figure 10, about 5%, 12.8%, 72%, and 29.5% of the SH demand is supplied by the electrical auxiliary heater, embedded in the SH tank, in January, March, November, and December, respectively.

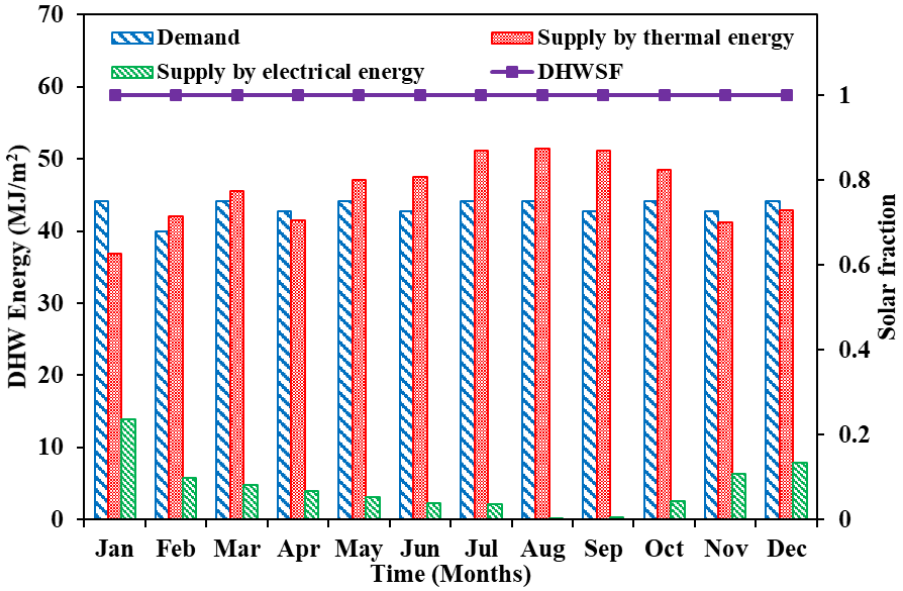

Figure 9. Monthly variations of DHW energy and DHWSF

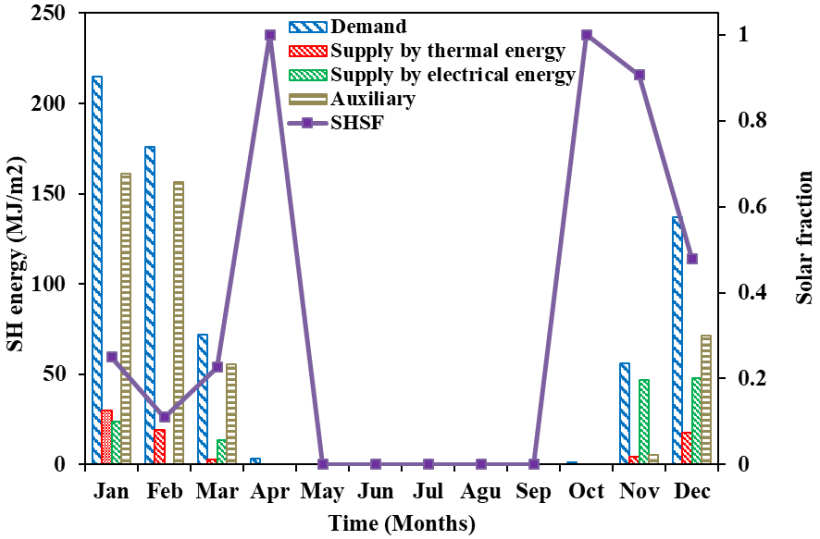

Figure 10. Monthly variations of SH energy and SHSF

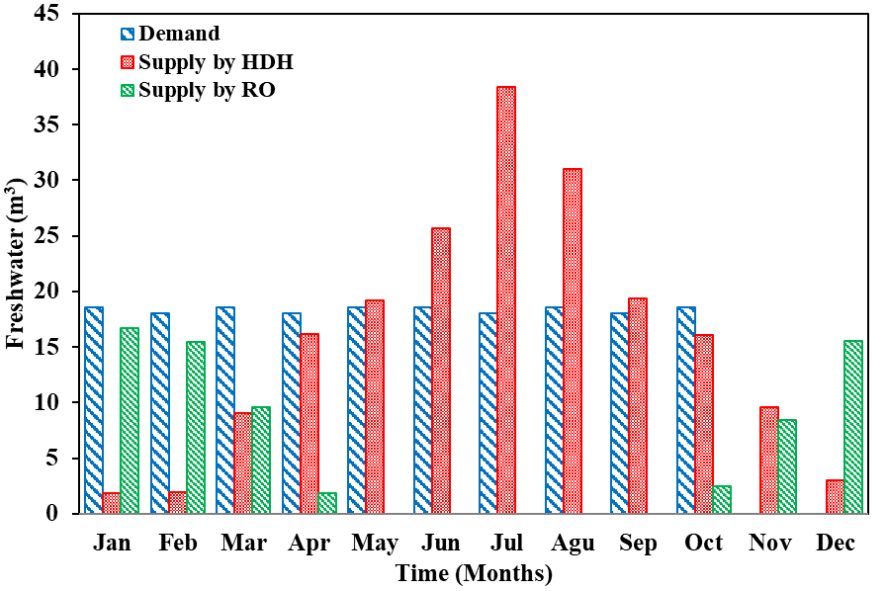

Figure 11. Monthly variations of freshwater demand and supply

Table 3. Performance indicators

Indicator	Electricity generation (kWh)	DHWSF (%)	SHSF (%)	DW generation (m^3) RO	HDH
Value	7907.4	100	27.2	70.1	191.4

Table 4. Results of life cycle cost analysis

Parameter	System cost, $/m^2	LCS for fuel saving cost ($)	LCS for water saving cost ($)	LCS for electricity sale ($)	LCS for water sale ($)	Payback period (year)
Value	5083.3	29479	23779	8158	1055	3.75

Figure 11 displays the monthly variations of the freshwater demand and supply by the hybrid HDH/RO units. The freshwater demand is determined based on the average daily water consumption per person, which is 150 lit [33]. As earlier mentioned, the electricity generation by PVT collectors is used to generate DW by RO unit, if the DW produced by the HDH unit is not enough. In warm months, from May to September, the DW produced by the HDH is higher than the freshwater demand; therefore, the DW production by the RO unit, and therefore, its electricity consumption is zero. In July, the DW production by the HDH is about 20.4 m^3 higher than the

freshwater demand, which is sold. The minimum and maximum DW production by the HDH is 1.9 m^3 in January and 38.4 m^3 in July. In January, which solar radiation is the lowest, the maximum DW production (16.7 m^3) by RO unit, and also its highest electricity consumption, is occurred, which is 85% higher than the DW production in October (2.5 m^3).

The annual performance indicators of solar polygeneration system are listed in Table 3. The annual DHWSF indicates that the required energy for DHW is completely provided by the PVT collectors, while about %73.8 of the SH demand should be provided by the auxiliary heater.

4. Economic analysis

In this study, the Life Cycle Cost (LCC) method is used to analyze the economic impacts of the proposed combisystem [34]. In this method, all the costs of the system over the lifetime are summed by taking into account the time value of money. In the present work, the economic scenario used is to receive no mortgage and pay 100% of the system's cost in advance. Therefore, the LCC, for a solar plus auxiliary system, was estimated by the following relation:

$$system\ cost\ =\ initial\ cost\ +\ fuel\ cost + parasitic\ energy\ cost + maintenance\ cost \quad (15)$$

The initial cost includes the equipment cost, design costs, transportation costs, installation costs, and the cost of the installation space if not installed on the roof of the building. The cost of equipment includes the cost of solar collectors, storage tanks, pumps, pipes, insulation, heat exchangers, and controllers. In this study, the PVT collector cost is 150 $\frac{\$}{m^2}$; therefore, by considering the collector area of 18 m^2, the initial cost of collectors is 2700 $[35]. The costs of the HDH and RO systems are considered 701.6 $ and 60 $, respectively. The total initial cost of the proposed system including the are-dependent and area-independent costs is 5083.3$.

The operational cost includes fuel cost, parasitic energy cost, and maintenance cost, which is considered as a percentage of the initial investment cost and increases annually at a certain rate. In this study, the system maintenance cost estimated initially at 1% of the initial system cost increased annually by 0.5% as the system ages [34].

The cost of the fuel consumed by the auxiliary heater is calculated using the following relation:

$$C_{AUX} = C_{FA} \int_0^t L_{AUX} dt \quad (16)$$

where C_{FA} is the cost rates ($/GJ) for auxiliary fuel.

The present worth (PW) of the system cost is expressed as:

$$PW_n = \frac{System\ Cost * (1+i)^{n-1}}{(1+d)^n} \quad (17)$$

where d = market discount rate, which is the reduction of the time value of money over time, and n is the number of life cycle years.

The Life Cycle Savings (LCS) is the difference between the cost of a solar system and the cost of a conventional system that works with fossil fuels:

$$System\ savings = fuel\ savings + water\ cost + resale\ value - extra\ parasitic\ energy\ cost - extra\ maintenance\ cost \quad (18)$$

where resale value is the cost of reselling system at the end of the system life which is considered 30% of the initial cost. The total present worth of the gains from the solar system compared to the fuel only system is also obtained using Eq. (17).

Another economic indicator, which is used for comparison of the systems, is the payback time. It is the time to return the initial capital of the time required for the annual solar savings to become positive [34]. In this study, the period of economic analysis is equivalent to the life of the system, which is taken as 20 years. The inflation rate and the discount rate are considered equal to Iran's economic indicators for 2016, which were respectively 9.6% and 15% [36]. The potable water and also, the energy carriers including the natural gas and electricity in Iran are subsidized by the Government; however, in this analysis, the non-subsidized global prices are considered. The natural gas, electricity and potable water prices are considered 0.77 $\frac{\$}{m^3}$, 0.15 $\frac{\$}{kWh}$ and 2.8 $\frac{\$}{m^3}$, respectively [37, 38]. The annual inflation rate of natural gas, electricity and potable water prices are expected to be 15%, 3% and 6%, respectively. The results of economic analysis are listed in Table 4. The total LCS of 62471 $ and the payback period of 3.75 years confirms that the proposed polygeneration system is an appropriate option to supply the energy demands of the houses in remote communities.

Conclusion

In this study, the thermal performance of the solar polygeneraion system integrating PVT collectors with hybrid HDH/RO units has been studied in Hot-Dry climate zone. The findings can be summarized as follows:

- By increasing the PV cell temperature, the collector electrical and thermal efficiency decreases to its minimum value at the maximum cell temperature between 12:30 and 13:30 pm. The maximum and minimum total PVT efficiencies are 62.8% at 13:30 pm and 70.3% at 4:00 pm.
- The maximum and minimum electricity generation is occurred in October and February, which are 863 kWh and 428.7 kWh, respectively. The higher electricity generation in the warm months is because of the higher solar irradiation.
- Using both thermal and electrical energy generated by the proposed system, the total DHW demand is supplied in all months.
- Using the proposed system, the SHSF of %11-%100 is obtained, which shows that the most fraction of the SH

required energy should be provided by the auxiliary heater. Due to assign the greater portion of the collector useful gain to supply DHW demand, the auxiliary energy for supplying the SH demand is always higher than that for DHW demand. In other words, DHWSF is higher than SHSF in all months.

- The minimum and maximum DW production by the HDH is 1.9 m^3 in January and 38.4 m^3 in July. The maximum DW production (16.7 m^3) by RO unit is occurred in January, which is 85% higher than that in October (2.5 m^3).
- By using the electrical energy generated for supplying the auxiliary energy needed for DHW and SH, the annual DHWSF and SH increases 11.3% and 15.6%, respectively.
- The economic analysis using LCC method showed that the cost saving of 62471 $ is achieved in the system lifetime and the payback time is 3.75 years.
- The results show that the considerable energy savings is achieved using the considered solar polygeneration system for providing the required thermal and electrical energy and freshwater demands of the residential buildings.
- Assumption of a fixed size for the collector and storage tanks is one of the limitations of this research, which can be studied in the next researches. Moreover, the required heating loads of the building can be calculated using more accurate software such as Design Builder. Furthermore, other types of SCSs including different configurations of the storage tanks and control strategies can be used in the proposed solar polygeneration system.

Nomenclature

C	Cost, $
c_p	Specific heat, kJ/kg K
C_{F1}	first year unit energy cost delivel from fuel
d	Discount rate
SF	Solar fraction
$\dot{H}$	Enthalpy rate (W)
h	Specific enthalpy J/kg
i_f	Fuel inflation rate
L	Load (J)
$\dot{m}$	Mass flow rate (kg/s)
n	Number of years
n_p	payback time
$\dot{Q}$	Heat transfer rate(KJ/h)
T	Temperature, K

Greek Symbols

ε	Effectiveness
ω	Absolute humidity, kg_w/kg_{da}

Subscripts

a	air
AUX	Auxiliary
D	Dehumidifier
da	Dry air
H	Humidifier
in	Intel
out	Outlet
max	Maximum
DW	Distilled water
w	Water

In General, the last paragraph of each paper is the place to acknowledge people and sponsors for dedicating and financial support. Company names and specific places should be cited only here. It should be noted that the heading of the Acknowledgment and the References must not be numbered.

Appendix

Appendixes appear after acknowledgments.

References

[1] Dehghan, M., Rahgozar, S., Pourrajabian, A., Aminy, M. and Halek, F.S., 2021. Techno-economic perspectives of the temperature management of photovoltaic (PV) power plants: A case-study in Iran. Sustainable Energy Technologies and Assessments, 45, 101133.

[2] Delfani, S. and Karami, M., 2020. Transient simulation of solar desiccant/M-Cycle cooling systems in three different climatic conditions. Journal of Building Engineering, 29, 101152.

[3] Good, C., Andresen, I. and Hestnes, A.G., 2015. Solar energy for net zero energy buildings – A comparison between solar thermal, PV and photovoltaic–thermal (PV/T) systems. Sol. Energy, 122, pp. 986-996.

[4] Sato, D. and Yamada,N., 2019. Review of photovoltaic module cooling methods and performance evaluation of the radiative cooling method. Renewable and Sustainable Energy Reviews, 104, 151-166.

[5] Dwivedi, P., Sudhakar, K., Soni, A., Solomin, E. and Kirpichnikova, I., 2020. Advanced cooling techniques of P.V. modules: A state of art. Case Studies in Thermal Engineering, 21, 100674.

[6] Jalalizadeh, M., Fayaz, R., Delfani, S., Jafari Mosleh, H. and Karami, M., 2021. Dynamic simulation of a trigeneration system using an absorption cooling system and building integrated photovoltaic thermal solar

collectors. Journal of Building Engineering, 43, 102482.
[7] Dupeyrat, P., Ménézo, C. and Fortuin, S., 2014. Study of the thermal and electrical performances of PVT solar hot water system. Energy Build., 68, pp. 751–755.
[8] Liang, R., Zhang, J. and Zhou, C., 2015. Dynamic Simulation of a Novel Solar Heating System Based on Hybrid Photovoltaic/Thermal Collectors (PVT). Procedia Eng., 121, pp. 675–683.
[9] Hazami, M., Riahi, A., Mehdaoui, F., Nouicer, O. and Farhat, A., 2016. Energetic and exergetic performances analysis of a PV/T (photovoltaic thermal) solar system tested and simulated under to Tunisian (North Africa) climatic conditions. Energy, 107, pp. 78–94.
[10] Hazami, M., Mehdaoui, F., Naili, N., Noro, M., Lazzarin, R. and Guizani, A. A. 2017. Energetic, exergetic and economic analysis of an innovative Solar CombiSystem (SCS) producing thermal and electric energies: Application in residential and tertiary households. Energy Convers. Manag., 140, pp. 36–50.
[11] Herrando, M., Ramos, A., Freeman, J., Zabalza, I. and N. Markides, C., 2018. Technoeconomic modelling and optimisation of solar combined heat and power systems based on flat-box PVT collectors for domestic applications. Energy Convers. Manag., 175, pp. 67–85.
[12] Elmnifi, M., Moria, H., Elbreki, A.M. and Abdulrazig, O.D.H., 2021. Possibilities Study of Using Hybrid Solar Collectors in Northeastern Libya Residential Home. International of Renewable Energy Research, 11 (2).
[13] Ahmadi, E., McLellan, B., Mohammadi-Ivatloo, B. and Tezuka, T., 2020. The Role of Renewable Energy Resources in Sustainability of Water Desalination as a Potential Fresh-Water Source: An Updated Review. Sustainability, 12, 5233.
[14] DeFelice, N.B. and MacDonald Gibson, J., 2013. Effect of domestic water use on air pollutant emissions in Abu Dhabi, United Arab Emirates. Int J Energy Environ Eng 4, 33.
[15] Bagheri, A., Esfandiari, N., Honarvar, B. and Azdarpour, A., 2020. An experimental study on the effects of direct and indirect use of solar energy on solar seawater desalination. Water Supply, 20 (1), pp. 259–268.
[16] Sohani, A., Hoseinzadeh, S. and Berenjkar, K., 2021. Experimental analysis of innovative designs for solar still desalination technologies; An in-depth technical and economic assessment. Journal of Energy Storage, 33, 101862.
[17] Abutayeh, M., Li, C., Yogi Goswami, D. and Stefanakos, E.K., 2014. Part V: Solar Desalination, Editor: Jane Kucera, Desalination: Water from Water. Scrivener Publishing, 551–582.
[18] Calise, F., Dentice d'Accadia, M. and Piacentino, A., 2014. A novel solar trigeneration system integrating PVT (photovoltaic/ thermal collectors) and SW (seawater) desalination: Dynamic simulation and economic assessment. Energy, 67, pp.1-20.
[19] Abbassi Monjezi, A., Chen, Y., Vepa, R., Kashyout, A.E.B., Hassan, G., Fath, H.E.B., Kassem, A.E.W. and Shaheed, M.H., 2020. Development of an off-grid solar energy powered reverse osmosis desalination system for continuous production of freshwater with integrated photovoltaic thermal (PVT) cooling. Desalination, 495, 114679.
[20] Alqaed, S., Mustafa, J. and Almehmadi, F.A., 2021. Design and Energy Requirements of a Photovoltaic-Thermal Powered Water Desalination Plant for the Middle East. Int. J. Environ. Res. Public Health, 18, 1001.
[15] Rabiee, H., Khalilpour, K.R., Betts, J.M. and Nigel Tapper, 2019. Chapter 13 - Energy-Water Nexus: Renewable-Integrated Hybridized Desalination Systems, Editor(s): Kaveh Rajab Khalilpour, Polygeneration with Polystorage for Chemical and Energy Hubs. Academic Press, pp. 409-458.
[22] Giwa, A., Fath, H. and Hasan, S.W., 2016. Humidification-dehumidification desalination process driven by photovoltaic thermal energy recovery (PV-HDH) for small-scale sustainable water and power production. Desalination, 377, pp.163–171.
[23] Hosseini, M. A. and Sarhaddi, F., 2017. Performance Assessment of a Humidification-Dehumidification Desalination Unit Connected to Photovoltaic Thermal Collectors. Amirkabir J. Mech. Eng., 49(3), pp. 653-662.
[24] Anand, B. and Srinivas, T., 2017. Performance evaluation of photovoltaic/thermal–HDH desalination system. Appl. Sol. Energy (English Transl. Geliotekhnika), 53 (3), pp.243–249.
[25] Mostafavi, S.M.H., Morteza Pour, H., Jafari Naeemi, K. and Shamsi, M., 2017. Experimental humidification-dehumidification desalination by concentrating photovoltaic/thermal solar collector. Biosystem. Eng., 49(3), pp. 295–305.

[26] Elsafi, A. M., 2017. Integration of humidification-dehumidification desalination and concentrated photovoltaic-thermal collectors: Energy and exergy-costing analysis. Desalination, 424, pp. 17–2.
[27] Gabrielli, P., Gazzani, M., Novati, N., Sutter, L., Simonetti, R., Molinaroli, L., Manzolini, G. and Mazzotti, M., 2019. Combined water desalination and electricity generation through a humidification-dehumidification process integrated with photovoltaic-thermal modules: Design, performance analysis and techno-economic assessment. Energy Convers. Manag. X, 1, 100004.
[28] Otanicar, T. and Qu, W., 2018. Thermodynamic analysis of hybrid humidification-dehumidification (HDH) - Reverse osmosis (RO) desalination system powered by concentrating photovoltaic/thermal solar collector. AIP Conf. Proc. 2033.
[29] Antoniadis, C. N. and Martinopoulos, G., 2019. Optimization of a building integrated solar thermal system with seasonal storage using TRNSYS. Renew. Energy, 137, pp. 56–66.
[30] Narayan, G. P., Sharqawy, M. H., Lienhard V, J. H. and Zubair, S. M., 2010. Thermodynamic analysis of humidification dehumidification desalination cycles. Desalin. Water Treat., 16 (1–3), pp. 339–353.
[31] Nawayseh, N. K., Farid, M. M., Omar, A. A. and Sabirin, A., 1999. Solar desalination based on humidification process - II. Computer simulation. Energy Convers. Manag., 40 (13), pp. 1441–1461.
[32] Narayan, G. P., McGovern, R. K., Zubair, S. M. and Lienhard, J. H., 2012. High-temperature-steam-driven, varied-pressure, humidification-dehumidification system coupled with reverse osmosis for energy-efficient seawater desalination. Energy, 37 (1), 482–493.
[33] Iranian National Building Code, Part 16: Sanitary Installations (2017).
[34] Kalogirou, S.A., 2014. Solar Energy Engineering: Processes and Systems. Second Edition, Elsevier Inc.
[35] https://www.alibaba.com/product-detai.
[36] Central Bank of the Islamic Republic of Iran.
[37] Tyra, B., 2019. Electric Power Monthly with Data. U.S. Energy Inf. Adm. (June), pp. 1–772.
[38] Rahaman, M. M. and Ahmed, T. S., 2016.Affordable Water Pricing for Slums Dwellers in Dhaka Metropolitan Area : The Case of Three Slums. J. Water Resour. Eng. Manag., 3 (1), pp. 15–33.